Journal of Materials Chemistry C

Chiral Inversion and Enhanced Cooperative Self-Assembly of Biosurfactant-Functionalized Porphyrin Chromsophores

Journal:	*Journal of Materials Chemistry C*
Manuscript ID	TC-COM-12-2019-006829.R1
Article Type:	Communication
Date Submitted by the Author:	24-Feb-2020
Complete List of Authors:	Peters, Kyle; Case Western Reserve University, Department of Physics Mekala, Shekar; Rensselaer Polytechnic Institute, Center for Biotechnology and Interdisciplinary Studies (CBIS) and New York State Center for Polymer Synthesis Gross, Richard; Rensselaer Polytechnic Institute, Center for Biotechnology and Interdisciplinary Studies (CBIS) and New York State Center for Polymer Synthesis Singer, Kenneth; Case Western Reserve University, Department of Physics

Chiral Inversion and Enhanced Cooperative Self-Assembly of Biosurfactant-Functionalized Porphyrin Chromophores

Kyle C. Peters,[*§a] Shekar Mekala,[§b] Richard A. Gross,[b] and Kenneth D. Singer[a]

[a] Department of Physics, Case Western Reserve University, Cleveland, OH, United States.
[b] Center for Biotechnology and Interdisciplinary Studies (CBIS) and New York State Center for Polymer Synthesis, Rensselaer Polytechnic Institute, Troy, NY, United States.

[§] Equal contributions
[*] Corresponding author: kcp24@case.edu

Abstract. A new self-assembling di-conjugated sophorolipid-(Zn)porphyrin was synthesized with a short lipid chain length connecting the porphyrin and disaccharide moieties in order to influence the self-assembled state. In dilute solution, circular dichroism measurements of the ordered molecules exhibited Cotton effects indicative of right-handed exciton-coupling; a chirality inversion compared to our previous report on (long-chain) sophorolipid-(Zn)porphyrins that formed a left-handed system. The self-assembly process was investigated by variable-temperature CD. Cooling curve profiles exhibited simultaneous evolution of net helicity and aggregation that corresponds with the cooperative assembly model. Analysis revealed a 3-fold increase in enthalpy of polymerization compared to long-chain species implying that shortening the distance between porphyrin and disaccharide moieties enhance the cooperative self-assembly. The morphology of assembled aggregates was examined by electron microscopy and showed mesoscopic cup-staked structures and nanofibrils.

In many self-organizing biological systems, the assembly process is mediated by a precise balance of non-covalent interactions involving, for example, π-π, hydrogen-bonding, steric and hydrophobicity.[1] An aim of supramolecular chemistry is to better understand and harness biological processes to fabricate advanced materials for applications spanning from drug delivery in modern medicine to novel functional (nano)materials and (opto)electronics.[2–7] Considering the latter, multi-chromophoric porphyrin systems show promise as candidates for next-generation organic electronics because of their efficient light harvesting and π-electron delocalization that facilitates charge transport.[8,9] A sustainable, biomimetic approach to gain efficient charge transport in porphyrin systems is to employ non-covalent interactions to drive self-assembly and control multi-chromophoric ordering—and our chosen approach for supramolecular polymerization is the biosurfactant sophorolipid. Sophorolipids (SL) were selected for conjugation to zinc (Zn) porphyrins because: (1) they bring important elements of natural self-assembly (hydrogen-bonding, steric and hydrophobic interactions),[10] (2) they are efficiency prepared (>250 g/L) by yeast fermentation and scalable,[11] all while (3) providing a tunable structure via facile chemo-enzymatic transformations[12] that permits us to map out the balance of non-covalent interactions.

In our recent report on the synthesis[13] and self-assembly[14] of di-conjugated SL-(Zn)porphyrin in dilute solution, it was found that hydrogen bond-bearing compounds polymerize into supramolecular structures having excess left-handed helical exciton-coupled J-type aggregates. We explored a number of SL-functionalized porphyrin compounds with differing structural features to tune the delicate non-covalent interactions that dictate the self-organization; namely, π-π stacking, hydrogen-bonding, steric and hydrophobicity. In this

communication, we report the synthesis and self-assembly behavior of a new SL-(Zn)porphyrin di-conjugate with a shortened hydrocarbon chain linker-length between the porphyrin core and peripheral disaccharide (**2C**, Fig. 1). Upon linker-length shortening (17 to 10 carbons) we found: (1) a chirality inversion of helical J-type exciton-coupled aggregates, and (2) a cooperative assembly enhancement with increased propensity to form a right-handed system.

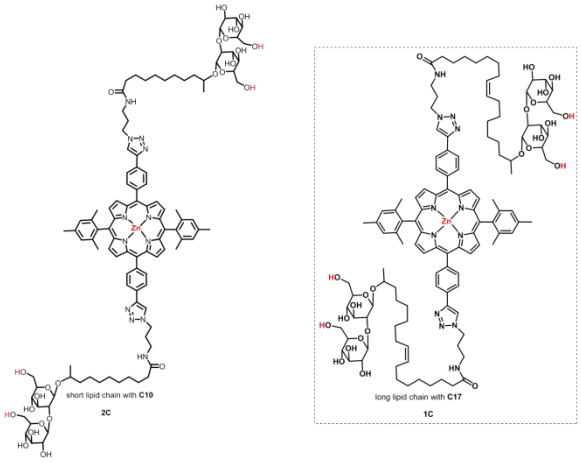

Fig. 1. Di-conjugated SL-(Zn)porphyrin short-chain compound (**2C**). In the dotted box, long-chain companion (**1C**). Details of synthetic methods for **2C** are given in the ESI†.

Control of chromophore-based chiral supramolecular structures in self-assembling systems have been demonstrated in sugar-substituted perylenediimide systems by variation of sugar stereochemistry,[15] solvent polarities,[16] spacer in perylene bisimide-carbohydrate conjugates,[17] and linker dependent control in porphryin-peptide conjugates.[18] From the perspective of biosurfactant amphiphilic systems, the chirality inversion phenomenon has only recently been observed in sorbitol-alkylamine by changing the hydrocarbon-chain linker length, which was attributed to twisting of the headgroup.[19] However, to the best of our knowledge, our team is the first to report chiral inversion with a sophorolipid-appended chromophore system.

We hypothesized that, by bringing the hydrogen-bonding disaccharide moiety closer to the porphyrin core the interactions between neighboring disaccharides of self-assembling SL-(Zn)Porphyrin conjugates may be amplified. In that, substantial changes in the conformation and orientation of SL-(Zn)Porphyrin conjugates will be required to achieve favorable energetics that drive self-assembly relative to its long-chain SL-(Zn)Porphyrin conjugate analogues (**1C**, Fig. 1).[20,21] We synthesized short-chain sophorolipid analogues from lactonic sophorolipid (LSL) by following previously published synthetic methods reported by our group as shown in Fig. 1.[22,23] Details of synthetic methods along with structural analysis (^{1}H NMR, ^{13}C NMR, HRMS, melting point) of products are given in the ESI†.

We reported compound **1C** (long-chain) self-assembles into helical J-type exciton-coupled aggregates with preferential left-handed screw sense in dilute MeOH:water (1:1 v/v, 3.0×10^{-6} M).[14] Herein, after the synthesis of **2C** (short-chain), spectroscopic CD, UV/vis absorption and emission studies were performed under the same experimental conditions as that for **1C**. Interestingly, the CD spectrum of **2C** showed an inverted chiroptic response compared to **1C** (Fig. 2a). That is, the CD spectrum of **2C** exhibited a trisignate +/-/+ Cotton effect (CE) signature with CE maxima at 442 nm (15 mdeg), 433 nm (-54 mdeg) and 421 nm (54 mdeg), respectively. In contrast, **1C** exhibited a -/+/- signature with CE maxima at 442 nm (-51 mdeg), 434 nm (62 mdeg) and 422 nm (-15 mdeg), respectively. Experimentally, CD represents the differential absorption between left- and right-handed circular polarized light ($\Delta\varepsilon = \varepsilon_L - \varepsilon_R$) and a spectral inversion about CD=0 arises from opposite handed chiral exciton coupling corresponding to an opposite helical screw sense.[24] Comparatively, the CE signature between **2C** (+/-/+) and **1C** (-/+/-) indicates chiral inversion from left-handed (**1C**) to a right-handed (**2C**)

system of J-type excitonically-coupled porphyrin chromophores. In addition to the spectral inversion, there appears to be a CE amplitude interchange between the first and third CEs compared to **1C**. We postulate this amplitude interchange arises from competition between nucleation of left- (M-type) and right-handed (P-type) aggregates and the differing propensities between the long- and short-chain compounds.

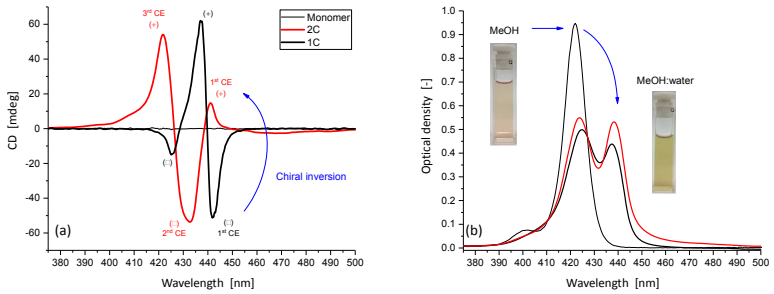

Fig. 2. Room temperature (a) CD and (b) UV/vis absorption measurements of compounds **2C** and **1C** in MeOH:water (1:1 vol. at 3.0×10^{-6} M).

The UV/vis absorption of compound **2C** was measured within the Soret region (Fig. 2b). The spectral lineshape exhibits a diminished optical density accompanied by the emergence of a split, red-shifted Soret band. Extinction maxima occur at 424 and 439 nm corresponding to an energy separation of about 800 cm^{-1}. In our earlier work,[13,14] we observed a similar response with compound **1C** (long-chain) and attributed the spectral lineshape change to the formation of slipped, co-facial J-type porphyrin aggregates. The presence of J-aggregates were further confirmed by photoluminescence measurements in MeOH and MeOH:water (Fig. S1, ESI†). Spectroscopic measurements of **2C** were also recorded in different MeOH/water-content mixtures (25%, 50%, and 75% water content) and showed optimal exciton coupling in a 1:1 MeOH:water 50% water content mixture (Fig. S2, ESI†), which is consistent with our previous reports on compound **1C**.[13,14] In addition, UV/vis and CD measurements in MeOH showed a CD-silent response accompanied by UV/vis absorption features consistent with non-interacting

porphyrin chromophores in solvent (Fig. S3, ESI†),[25,26] indicating a monomeric (fully dissolved) state.

Temperature interval UV/vis (Fig. 3a) and CD (Fig. 3b) spectral scans were performed by slow cooling a dilute solution from elevated temperatures. At 50 ˚C, the UV/vis Soret region of **2C** returned to a single absorption band located at 422 nm, a 1 nm red-shift compared to the monomeric state in MeOH (Fig. S3, ESI†). Upon slow cooling, the red-shifted J-aggregate UV/vis band emerges near 439 nm, meanwhile the high energy band near 422 nm subsides (Fig. 3a). Concurrently, the CD scans (Fig. 3b) show CE band growth to maximum values of 71 mdeg (422 nm), -79 mdeg (432 nm) and 22 mdeg (441 nm) from an optically inactive (CD=0) state at 50 ˚C. The temperature interval spectral trends presented here suggest a thermally active equilibrium polymeric system,[27] much like its long-chain analogue **1C**.[14] To elucidate the thermally active self-assembly process, temperature-dependent cooling curves were recorded by monitoring the spectral band evolution at fixed wavelength. Per our earlier work,[14] λ_{probe} = 442 nm was chosen such that both CD and UV/vis band evolution can be monitored simultaneously. Upon data normalization to unity (see ESI†), the CD and UV/vis cooling curves represent the system's net helicity and degree of aggregation, respectively, as a function of temperature.

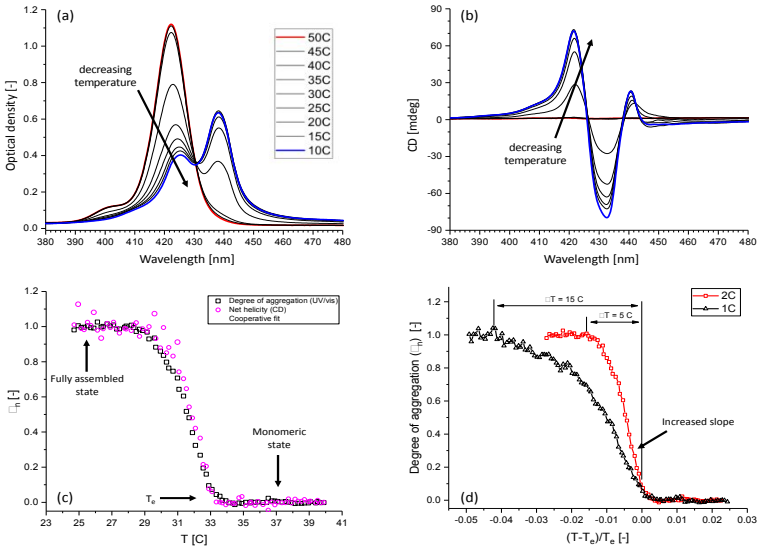

Fig. 3. Variable-temperature measurements for **2C** at 3.0×10^{-6} M recorded in MeOH:water (1:1 v/v). (a) UV/vis and (b) CD temperature interval (5 ˚C) scans while slow cooling (2 ˚C min^{-1}) from 50 ˚C with 2-minute settling time. (c) Normalized degree of aggregation (UV/vis) and net helicity (CD) profile of **2C** during slow cooling (1 ˚C min^{-1}) monitored at 442 nm. (d) Normalized degree of aggregation (UV/vis) curve profile of **2C** and **1C** as a function of reduced temperature, $(T-T_e)/T_e$, highlighting the cooperative polymerization enhancement monitored at 442 nm.

Plots for **2C** of net helicity (CD) and degree of aggregation (UV/vis) vs temperature (Fig. 3c) exhibit exponential trends (non-sigmoidal) that are superimposable, indicating similar nucleation-elongation (cooperative) self-assembly.[28,29] This result is in sharp contrast to our earlier work with **1C** (long-chain), where we observed that aggregation (UV/vis) and preferential formation of one helical sense (CD) were not coupled during the supramolecular polymerization.[14] That is, **1C** showed a linear net helicity (CD) cooling curve profile that did not plateau at low temperature in comparison to the degree of aggregation (UV/vis) that exhibited an exponential profile with a plateau at low temperatures. We postulated that this discrepancy arose from a competition between nucleation of left- (M-type) and right-handed (P-type) aggregates, thereby producing a net helicity curve that is non-exponential (i.e., linear). Here, Fig. 3c clearly shows the net helicity and degree of aggregation are similar, which suggests that

aggregation and preferential helical sense are coupled during the supramolecular polymerization of **2C**.[29,30] In tandem with the CD amplitude interchange observed earlier (Fig. 2a), we suspect the presence of the long lipid chain decreases the propensity to self-assemble by permitting parasitic flexibility and steric effects.

By simultaneously applying a modified nucleation-elongation model (eq. S2 and S3)[28,29] on **2C**'s UV/vis and CD cooling curves (Fig. S4, ESI†), the onset of polymerization, i.e. the elongation temperature (T_e) was determined to be 305.9 K (32.75 ˚C). Also, the activation equilibrium constant (K_a) and average enthalpy release of non-covalent interactions upon elongation (h_e) are 6.07 ± 1.61 × 10^{-4} and -494.8 ± 19.8 kJ mol^{-1}, respectively. The enthalpy of elongation (h_e) value for **2C** is over 3-fold larger compared to its long-chain analogue **1C** that we reported in earlier work under identical conditions (i.e., -140 kJ mol^{-1}).[14] Moreover, it is known that the slope of the cooling curve near the elongation temperature is proportional to the enthalpy,[27] which facilitates the assembly rate. Observation of the degree of aggregation curves in Fig. 3d reveals that, the self-assembly process for **2C** occurs more rapidly. The cooling curve reaches a plateau (fully assembled state) in only about a 5 ˚C temperature differential from the onset of polymerization (T_e) for **2C**, as compared to about 15 ˚C for the long chain analogue **1C**. To further elucidate how shortening the distance between the porphyrin and disaccharide moieties influence the structures formed by self-assembly, morphology studies were carried out.

The morphology of self-assembled structures formed by **2C** was investigated by electron microscopy using both scanning (SEM) and transmission (TEM). The SEM image (Fig. 4a) reveals the formation of mesoscopic aggregates that appear as elongated stacks of cups. TEM images

(Fig. 4b and 4c) revealed that **2C** forms clumped aggregates composed of nanofibers, which is very similar to that observed in our previous report on long-chain **1C**.[14] The remarkable aggregated structures associated with the short-chain compound reflects the robust and rapid assembly process compared with the long-chain compound. Additional electron microscopy images of **2C** can be found in the ESI† (Fig. S5 and S6, ESI†). Although higher magnification TEM images were unobtainable, we speculate that the fibrillar oligomers observed in Fig. 4b and 4c consist of helical J-type arranged excitonically-coupled porphyrin chromophores while the mesoscopic aggregates in Fig. 4a indicates the formation of higher ordered structures. However, further investigations into aggregate morphology is needed and additional experiments are the focus of future work.

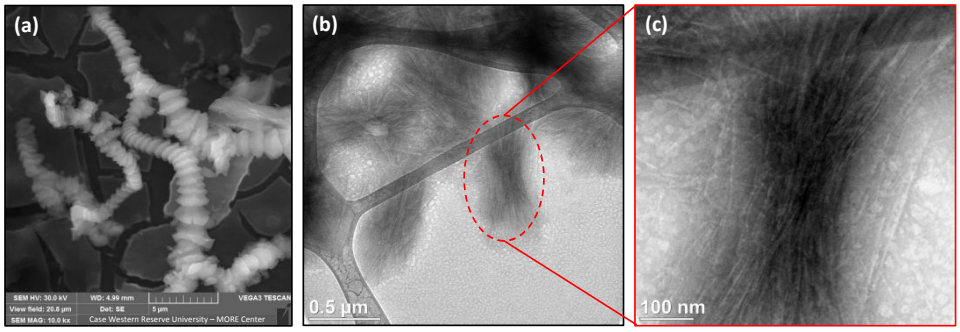

Fig. 4. Electron microscopy images of **2C** recorded in the solid state. (a) SEM image captured at 10.0 kx, samples were casted from a 1 mg mL^{-1} solution. TEM images captured at (b) 11.5 kx and (c) 42.0 kx, samples were prepared from a 0.5 mg mL^{-1} solution.

In summary, we synthesized a new di-conjugate sophorolipid-(Zn)porphyrin compound (**2C**) that was designed to shorten the linker-length between the porphyrin core and peripheral disaccharides. This structural modification, relative to its longer chain analogue (**1C**), caused a chiral reversal that was realized by an inverted CD spectrum in dilute MeOH:water (1:1 v/v) solution. The reversal resulted in a right-handed excitonically-coupled helical system of J-type aggregates, in contrast to our recent report on its long-chain companion **1C** that formed a left-

handed system. In addition, the combination of ^{1}H NMR, ^{13}C NMR, HRMS, melting point and UV-vis shows unequivocally that the synthesized compounds are highly pure, thus ruling-out impurities as the cause of chiral inversion. Considering that steric interaction contributes to the generation of self-organized chiral ensembles as well as intermolecular hydrogen-bonds and π-π, we speculate that steric reduction aids in the chiral inversion facilitation, however, further investigation into the inversion mechanism is the focus of future work. Temperature-dependent self-assembly studies of **2C** revealed that aggregation (UV/vis) and preferential formation of one helical sense (CD) are coupled during the supramolecular polymerization in contrast to the long-chain analogue **1C**. Cooling curves of **2C** are well-described by a nucleation-elongation model with an enthalpy of elongation that is over 3-fold larger than **1C**, which reflects a more energetically favorable assembling system for **2C**–i.e. a cooperative self-assembly enhancement. TEM images displayed clustering of fibril aggregates and SEM images revealed mesoscopic cup-stacked aggregates. The highly malleable structure of sophorolipids achieved by simple chemo-enzymatic modification methods along with its efficient synthesis by yeasts provides a unique platform to manipulate important elements that control self-assembly (e.g., hydrogen-bonding and amphiphilic character). This work validates how variation in sophorolipid structure, in this case by changing the linker length separating sophorose and porphyrin moieties that assemble by hydrogen-bonding and π-π interactions, respectively, permits dramatic changes in the propensity for self-assembly as well as the structures formed, and future work involving systematic changes in linker length could further our knowledge of structure-assembly correlations. This validates the possibility of using complex abundant glycolipids as a means to manipulate the organization of π-extended chromophores as well as

other functionalities to develop next-generation nanoarchitectures for optofunctional applications.

Experimental section

See the Electronic Supporting Information

Conflicts of interest

There are no conflicts to declare

Associated content

Electronic Supporting Information. Synthesis and chemical characterization, spectroscopic and microscopy methods, additional measurements including photoluminescence and UV/vis, CD, cooling curve model and fitting, additional electron microscopy images.

Acknowledgements

Financial support from NSF Program for International Research and Education (PIRE), grant: OISE-1243313 is gratefully acknowledged. The authors acknowledge the use of the Materials for Opto/electronics Research and Education (MORE) Center (Ohio Third Frontier grant TECH 09-021), the Swagelok Center for Surface Analysis of Materials (SCSAM) at Case Western Reserve University for SEM and TEM imaging, and the Molecular Biotechnology Core at the Cleveland Clinic Foundation - Lerner Research Institute for use of the JASCO CD spectrophotometer.

References

1 A. R. A. Palmans and E. W. Meijer, *Angew. Chemie Int. Ed.*, 2007, **46**, 8948–8968.
2 J. D. Tovar, *Acc. Chem. Res.*, 2013, **46**, 1527–1537.
3 N. Koch, *Supramolecular Materials for Opto-Electronics*, Royal Society of Chemistry, 2014.
4 M. A. Rajora, J. W. H. Lou and G. Zheng, *Chem. Soc. Rev.*, 2017, **46**, 6433–6469.
5 S. Zhang, *Nat. Biotechnol.*, 2003, **21**, 1171.
6 M. Liu, L. Zhang and T. Wang, *Chem. Rev.*, 2015, **115**, 7304–7397.
7 L. Zhang, T. Wang, Z. Shen and M. Liu, *Adv. Mater.*, 2016, **28**, 1044–1059.
8 M. Jurow, A. E. Schuckman, J. D. Batteas and C. M. Drain, *Coord. Chem. Rev.*, 2010, **254**, 2297–2310.
9 L. Smykalla, C. Mende, M. Fronk, P. F. Siles, M. Hietschold, G. Salvan, D. R. T. Zahn, O. G. Schmidt, T. Rüffer and H. Lang, *Beilstein J. Nanotechnol.*, 2017, **8**, 1786.

10 S. Zhou, C. Xu, J. Wang, W. Gao, R. Akhverdiyeva, V. Shah and R. Gross, *Langmuir*, 2004, **20**, 7926–7932.
11 V. Guilmanov, A. Ballistreri, G. Impallomeni and R. A. Gross, *Biotechnol. Bioeng.*, 2002, **77**, 489–494.
12 S. K. Singh, A. P. Felse, A. Nunez, T. A. Foglia and R. A. Gross, *J. Org. Chem.*, 2003, **68**, 5466–5477.
13 S. Mekala, K. C. Peters, K. D. Singer and R. A. Gross, *Org. Biomol. Chem.*, 2018, **16**, 7178–7190.
14 K. C. Peters, S. Mekala, R. A. Gross and K. D. Singer, *ACS Appl. Bio Mater.*, 2019, **2**, 1703–1713.
15 X. Liu, Z. Huang, Y. Huang, L. Zhu and J. Fu, *J. Phys. Chem. C*, 2017, **121**, 7558–7563.
16 Q. Guo, J. Wang, L. Zhu and Z. Wei, *Chinese J. Chem.*, 2015, **33**, 95–100.
17 K.-R. Wang, D. Han, G.-J. Cao and X.-L. Li, *RSC Adv.*, 2015, **5**, 47728–47731.
18 F. Biscaglia, E. Frezza, E. Zurlo and M. Gobbo, *Org. Biomol. Chem.*, 2016, **14**, 9568–9577.
19 P. Zhang, J. Ma, X. Kang, H. Liu, C. Chen, Z. Zhang, J. Zhang and B. Han, *Chem. Commun.*, 2017, **53**, 2162–2165.
20 S. I. Tamaru, M. Nakamura, M. Takeuchi and S. Shinkai, *Org. Lett.*, 2001, **3**, 3631–3634.
21 S. Kawano, S. Tamaru, N. Fujita and S. Shinkai, *Chem. Eur. J.*, 2004, **10**, 343–351.
22 Y. Peng, F. Totsingan, M. A. R. Meier, M. Steinmann, F. Wurm, A. Koh and R. A. Gross, *Eur. J. Lipid Sci. Technol.*, 2015, **117**, 217–228.
23 K. S. Bisht, R. A. Gross and D. L. Kaplan, *J. Org. Chem.*, 1999, **64**, 780–789.
24 N. Berova, L. Di Bari and G. Pescitelli, *Chem. Soc. Rev.*, 2007, **36**, 914–931.
25 M. Gouterman, *J. Mol. Spectrosc.*, 1961, **6**, 138–163.
26 M. Gouterman, G. H. Wagnière and L. C. Snyder, *J. Mol. Spectrosc.*, 1963, **11**, 108–127.
27 P. Van der Schoot, in *Supramolecular polymers*, CRC Press, Boca Raton, FL, 2005, pp. 77–106.
28 P. Jonkheijm, P. van der Schoot, A. P. H. J. Schenning and E. W. Meijer, *Science*, 2006, **313**, 80–3.
29 M. M. J. Smulders, A. P. H. J. Schenning and E. W. Meijer, *J. Am. Chem. Soc.*, 2008, **130**, 606–611.
30 S. Cantekin, D. W. R. Balkenende, M. M. J. Smulders, A. R. A. Palmans and E. W. Meijer, *Nat. Chem.*, 2011, **3**, 42–46.

Graphical Abstract

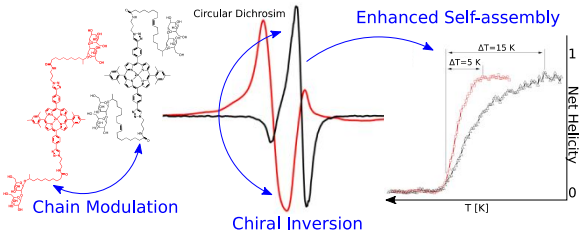

Table of Contents Entry

A newly synthesized sophorolipid-(Zn)porphyrin (short lipid chain) exhibits chiral inversion and

enhanced cooperative self-assembly compared to its analogue long-chain compound.